Structural Anomalies and Multiferroic Behavior in Magnetically Frustrated $TbMn_2O_5$

L. C. Chapon,[1] G. R. Blake,[1,2] M. J. Gutmann,[1] S. Park,[3] N. Hur,[3] P. G. Radaelli,[1] and S-W. Cheong[3]

[1]*ISIS Facility, Rutherford Appleton Laboratory-CCLRC, Chilton, Didcot, Oxfordshire, OX11 0QX, United Kingdom*

[2]*Materials Science Division, Argonne National Laboratory, Argonne, Illinois 60439, USA*

[3]*Department of Physics and Astronomy, Rutgers University, Piscataway, New Jersey 08854, USA*

(Received 15 April 2004; published 18 October 2004)

We have studied the magnetostructural phase diagram of multiferroic $TbMn_2O_5$ as a function of temperature and magnetic field by neutron diffraction. Dielectric and magnetic anomalies are found to be associated with steps in the magnetic propagation vector, including a rare example of a commensurate-incommensurate transition on cooling below 24 K, and in the structural parameters. The geometrically frustrated magnetic structure is stabilized by "canted antiferroelectric" displacements of the Mn^{3+} ions, an example of the magnetic Jahn-Teller effect. The Tb moments order ferromagnetically at low temperatures in an applied field, while the Mn magnetic structure is largely unchanged.

DOI: 10.1103/PhysRevLett.93.177402 PACS numbers: 78.70.Nx, 75.25.+z, 77.80.–e

Compounds with the general formula RMn_2O_5 (R = La, Y, rare earth, or Bi) have been studied since the late 1960's for their unusual magnetic properties [1–4]. These insulators all order antiferromagnetically below 50 K with a propagation vector $(kx, 0, kz)$, with $kx \sim \frac{1}{2}$ [**k** values are given in reciprocal lattice units (r.l.u.)]. kz varies between 0 and 0.5, displaying a remarkable dependence on the size of the R-site cation and on temperature. This is related to the complexity of the RMn_2O_5 crystal structure, where $Mn^{4+}O_6$ octahedra and $Mn^{3+}O_5$ pyramids are linked through edge- and corner-sharing networks, leading to five independent nearest-neighbor (NN) magnetic interactions. Several studies of dielectric and magnetoelectric properties have indicated that RMn_2O_5 compounds are ferroelectric in their magnetically ordered state [5,6], the spontaneous polarization **P** being directed along the b axis [6]. These measurements also evidenced several transitions in both dielectric constant and polarization, and it has long been speculated that these may be related to magnetic transitions. A linear magnetoelectric signal has also been evidenced in $TbMn_2O_5$ below 10 K, indicating that macroscopic time reversal symmetry is broken upon R-site magnetic ordering [5]. These compounds are very unusual, in that $|\mathbf{P}|$ is much smaller than in typical ferroelectrics and there is very little evidence of structural transitions [6]. The mechanism leading to the development of a spontaneous polarization has not yet been clarified. Very recently, Hur and co-workers have shown an even more striking correlation between the magnetic and electric properties of $TbMn_2O_5$ [7]: **P** and the dielectric constant ϵ undergo four separate transitions, associated with anomalies in the magnetic susceptibility, a remarkable display of multiferroic behavior [8]. The direction of **P** can be reversed by applying a magnetic field H at low temperatures, and a permanent imprint is left in the polarization. In this Letter, we report neutron diffraction measurements on $TbMn_2O_5$ as a function of T and H which show unambiguous correlations between dielectric anomalies and changes in the periodicity of the spin structure. First, the onset of ferroelectricity at 38 K is associated with the appearance of incommensurate antiferromagnetic (AFM) ordering $T_1 = 43$ K. At $T_2 = 33$ K, just above the maximum in **P**, **k** locks into a commensurate value $(\frac{1}{2}, 0, \frac{1}{4})$. Remarkably, at $T_3 = 24$ K, where ϵ has an upward "jump," **k** becomes suddenly incommensurate again, a rare example [9,10] of such a transition on *cooling*. The low-temperature transition ($T_4 = 10$ K) coincides with a major increase of the Tb ordered moment. The 43 and 24 K transitions are accompanied by clear anomalies in the lattice parameters, particularly along the b "polar" axis, and in the atomic displacement parameters (ADPs). Our magnetic structure solution for the commensurate phase strongly suggests that $TbMn_2O_5$ is a realization of the AFM square lattice with asymmetric next-nearest-neighbor (NNN) interactions, a simple geometrically frustrated system [11]. In this scenario, small structural displacements would lift the magnetic degeneracy and reduce the exchange energy, an example of the so-called magnetic Jahn-Teller effect [12]. The direction of the observed macroscopic polarization (along the b axis), is a direct consequence of the magnetic symmetry. The unusually small $|\mathbf{P}|$ would result from a "canted antiferroelectric" arrangement of the displacement vectors. Upon application of a magnetic field, Tb orders ferromagnetically at low temperatures, while the AFM structure of the Mn sublattices is largely unchanged. Based on these results, we propose a comprehensive explanation of the T and H dependence of **P**.

Polycrystalline $TbMn_2O_5$ was prepared through conventional solid-state reaction in an oxygen environment. Single crystals of $TbMn_2O_5$ (typical size 10 mm^3) were grown using B_2O_3-PbO-PbF_2 flux in a Pt crucible. Neutron powder and single-crystal diffraction data were collected using the GEM and SXD diffractometers at the

ISIS facility. For the powder experiment, a helium cryostat and a superconducting cryomagnet were employed. Single-crystal data were collected at 27 K, using a closed-cycle refrigerator. Magnetic and structural refinements (space group *Pbam*), were performed with the programs FullProF and GSAS, respectively [13]. The dielectric constant was measured at 1 kHz using an *LCR* meter. The polarization was calculated by integrating the measured pyroelectric current. Before each pyroelectric current measurement, the sample was cooled from 120 to 3 K in a static electric field, $E_{-}\text{pole} = 4\text{kV/cm}$ and zero magnetic field.

The main features of the magnetic phase diagram of $TbMn_2O_5$ are clearly associated with electric anomalies as summarized in Fig. 1. Magnetic order is first observed at $T_1 = 43$ K with an incommensurate propagation vector $\mathbf{k}$ ($\sim 0.50, 0, 0.30$). The growth of magnetic Bragg peaks is mirrored by a decrease of the paramagnetic background. The discommensuration is suppressed at 33 K where $\mathbf{k}$ locks at $(\frac{1}{2}, 0, \frac{1}{4})$. Remarkably, at 24 K, both kx and kz suddenly jump to incommensurate values (0.48, 0, 0.32). The increase of the intensity of all the magnetic Bragg peaks and a further suppression of the background clearly indicate that additional magnetic ordering takes place at the 24 K transition. Finally, below 10 K, the magnetic Bragg peaks become much more intense and the background is fully suppressed due to a large ordered moment on the Tb sublattice.

The evolution of the lattice parameters and of the Mn ADPs as a function of temperature is shown in Fig. 2. Small but distinct lattice anomalies, leading to linear changes $\Delta l/l$ of the order of 10^{-4}, are evident at 43 and 24 K. Interestingly, the anomalies are larger along the b axis, which is the direction of the spontaneous polarization. These anomalies are clearly of exchange-strictive origin: The ADP of Mn^{3+} displays a significant increase into the magnetic phase, indicative of structural displacements, while that of Mn^{4+} is normal. Also, the ADPs of Tb and one of the O atoms [O(2) linking adjacent Mn^{4+} octahedra along the c axis] show a pronounced increase on cooling, strongly suggesting that they contribute to the ferroelectric polarization, at least at low temperatures. All these sites would be split in the proposed $Pb2_1m$ polar group [6]. However, no new nuclear Bragg peaks appear below T_1 in either our powder or single-crystal data, indicating that the polar component of these displacements is very small.

To date, the magnetic structures in RMn_2O_5 have been ascribed either to the helimagnetic [1] or to the spin density wave (SDW) [2,3] types. This complexity was attributed to the presence of various competing exchange interactions (Fig. 3, inset). Along c, Mn^{4+} atoms interact via direct exchange and weak superexchange with two inequivalent interactions (J_1, through the R layer, J_2 through the Mn^{3+} layer). The Mn^{4+} interacting through J_2 are also linked to $Mn^{3+}O_5$ pyramids either through their pyramidal base corners (J_3) or through the pyramid apex (J_4). J_3 and J_4 are both of the superexchange type and are controlled by Mn^{4+}-O-Mn^{3+} bond angles ($\sim 123°$ for J_3 and $\sim 131°$ for J_4), distinct but both close to the FM/AFM crossover [14]. Finally, the pyramids are linked together by their base edges (J_5). The competition between Mn^{4+}-Mn^{4+} superexchange interactions (J_2 vs J_3/J_4) is an obvious ingredient for complexity as J_3 and J_4 always tend to align the Mn^{4+} *parallel* to each other, whatever their sign, whereas an AFM $J_2 > 0$ would have the opposite effect. For large enough J_2, a helimagnetic

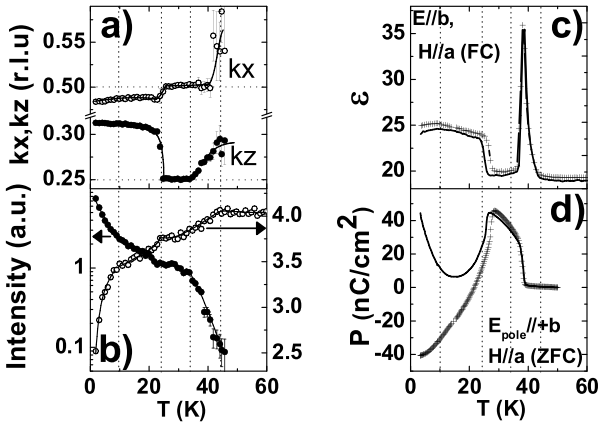

FIG. 1. Phase diagram of $TbMn_2O_5$. (a) Propagation vector components along a^* (open circle) and c^* (filled circle). (b) Integrated intensity of the (100)-$\mathbf{k}$ reflection (filled circle) and background level integrated over $0.76 < Q < 0.87$ Å^{-1} (open circles). Dielectric constant [panel (c)] and spontaneous polarization [panel (d)] in zero magnetic field (solid line) and 3 T (cross symbol) (see Ref. [7] for details). Vertical dotted lines mark the transition temperatures (see text).

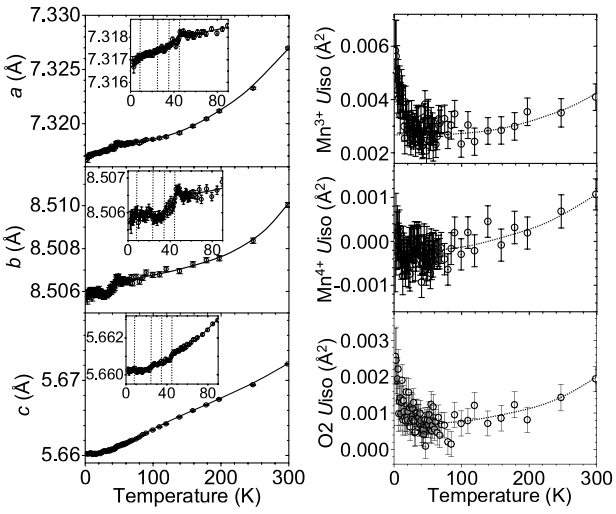

FIG. 2. Temperature dependence of selected structural parameters. Left panel represents variation of lattice parameters. Right panel shows an equivalent atomic displacement parameter for selected atoms. Lines are guides to the eye.

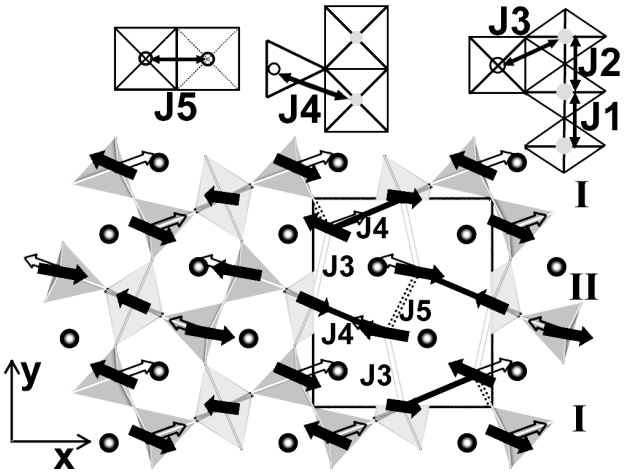

FIG. 3. Refined magnetic structure (black arrows) and proposed polar displacements (white arrows) at 27 K. The refined magnetic moments of 1.81 and 2.40 μ_B for Mn^{4+} and Mn^{3+} are significantly lower than the expected fully ordered spin values, indicating that a significant component of the moment remains disordered. The canting angles with respect to the *a* axis are of 24° and 10°. The *c*-axis stacking of these layers can be interpreted as a pure $\ldots + + - - + + - - \ldots$ sign modulation. Through the Tb layer, the coupling alternates between AFM (as in $BiMn_2O_5$) and FM (as in $DyMn_2O_5$). A small induced moment on Tb (1.6 μ_B) is present with the FM interlayer coupling and absent for the AFM one. This detail is essential to obtain a perfect fit of the data (Fig. 4), but the refinement is rather insensitive to the moment orientation. The Tb moment is omitted in the drawing for clarity. Roman numerals refer to the *a*-axis AFM chains (see text).

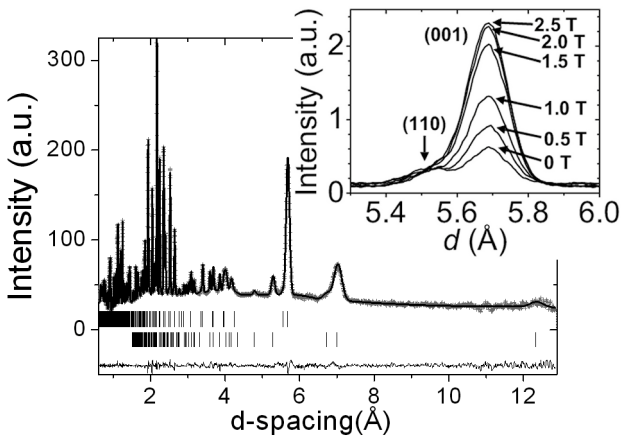

FIG. 4. Rietveld refinement pattern for $TbMn_2O_5$ at 27 K. The data from three banks of detectors have been grouped on a common scale. The top and bottom rows of tick marks refer to nuclear and magnetic reflections, respectively. The inset shows the field dependence of a nuclear peak at 1.5 K.

structure may be stabilized [4]. However, none of the magnetic structures reliably determined to date are helimagnetic. The commensurate phases of $DyMn_2O_5$ [2] and $BiMn_2O_5$ [4], and the incommensurate SDW structures of $TbMn_2O_5$ at 1.5 K and of $ErMn_2O_5$ (at 4 and 25 K) [3], are all noncollinear AFM. It is interesting to compare these structures with the present *commensurate* $(\frac{1}{2}, 0, \frac{1}{4})$ problem. As in the incommensurate case [3], each of the magnetic atoms in the unit cell is allowed to have an independent SDW, i.e., its own amplitude and phase. However, one would strongly suspect to find a simple set of phase relations. Uniquely, $kz = \frac{1}{4}$ can lead to a sign modulation without a spin amplitude modulation. To solve the magnetic structure, a simulated annealing algorithm was used with single-crystal data to search for starting configurations. The phases were then fixed while the magnitude and directions of the moments were refined by Rietveld analysis of the powder data (Fig. 4), which are more complete at low momentum transfer, using constant-moment analysis [4] (Fig. 3, see caption for details). As expected, the phase relations are simple and consistent with a pure sign modulation of the Mn sites: all the Mn^{4+} and Mn^{3+} waves have the same phase, while Tb has a phase shift of $\pi/4$. The moments are in the *ab* plane, predominantly along the *a* direction. The magnetic structure of the Mn^{3+}/Mn^{4+} layers is very similar to that of $BiMn_2O_5$ or $DyMn_2O_5$. This suggests a stable magnetic arrangement of the Mn^{4+}/Mn^{3+} layers: Mn^{4+} ions are always coupled *ferromagnetically* along the *c* axis ($|J_2| \ll |J_3|$ and $|J_2| \ll |J_4|$), and form AFM $\ldots Mn^{4+}$-Mn^{3+}-Mn^{3+}-$Mn^{4+}\ldots$ chains along the *a* axis ($|J_4| > |J_3|$, $J_4 > 0$, and $J_5 > 0$). However, the *R* ionic radius "tunes" the magnetic interaction J_1, so that $J_1 < 0$ for Dy, $J_1 > 0$ for Bi, and J_1 alternates >0 and <0 for Tb. The anomalous ADPs observed for the Tb and O(2) atoms could indicate that weak fluctuations in bond lengths along the chain cause the modulation of the exchange integral sign as direct exchange and superexchange compete. With this hierarchy of interactions, the Mn^{4+} sublattice maps to a very simple system: the square lattice with asymmetric NNN interactions. In this scheme, the NN interactions are conveyed by J_3 and J_4 and are FM or AFM, depending on the sign of J_3. The NNN interaction along the *a* axis (through J_4 and J_5) is stronger than the one along the *b* axis (through J_3 and J_5), so that AFM chains along the *a* axis are always stabilized. This is clearly a geometrically frustrated system: two out of the four magnetic links around each Mn^{4+} have the wrong sign, whatever the sign of J_3, leading to exact cancellations of exchange energy terms. A small structural distortion would naturally lift this magnetic degeneracy, leading to a reduction of the exchange energy, as speculated by Kagomiya [6]. Magnetic interactions with the "right" and the "wrong" sign would be strengthened or weakened, respectively, by a modulation of the Mn^{4+}-O-Mn^{3+} bond angles, a realization of the so-called magnetic Jahn-Teller effect [12]. The allowed direction of **P** can be unambiguously determined by symmetry analysis. None of these phases can be described within the Schubnikov formalism, but one can still establish that, for the proposed modes, the magnetic

point group is $m2m1'$, which is *only* compatible with a b axis polar vector, as in the proposed polar space group $Pb2_1m$ [6]. A possible pattern for the case $J_3 > 0$, involving Mn^{3+} displacements along the axis of the pyramids, is shown in Fig. 3. Although the displacements are along a general crystallographic direction in the ab plane, the a-axis component cancels out identically, while the smaller b-axis component does not. This "canted antiferroelectricity" is the dielectric analogue of weak ferromagnetism arising from a canted AFM arrangement. Our field-dependent data (inset to Fig. 4) provide further insight into the complex field and temperature dependence of **P**. In an applied field of 2.5 T the Tb moments order ferromagnetically with a dominant a-axis component, in agreement with the magnetization data [7]. However, the magnetic structure of the Mn sublattice is essentially the same at 15 K/$H = 0$ T and at $T =$ 1.5 K/$H = 2.5$ T. This can be shown by subtracting the 15 K zero-field data from the 1.5 K, 2.5 T data, leaving an essentially perfect ferromagnetic pattern. Also, **k** is unaffected by the field. These results, together with the observation that the field effect on **P** is the same regardless of the *sign* of H (along the a axis) [7], lead one to conclude that the main effect of H is to *suppress* the Tb contribution to **P**, as its moments are aligned FM. In high field, one would measure the pure contribution to **P** of the other sublattices; its temperature dependence indicates that **P** *changes sign* at the commensurate-incommensurate transition (Fig. 1). YMn_2O_5 undergoes an analogous polarization reversal at 20 K [6], strongly supporting this interpretation. This remarkable effect can be understood by the concept of coherent superposition of different "regions." Within each Mn^{3+}/Mn^{4+} layer, there are 4 possible magnetic configurations, which can be obtained by reversing one (I or II) or both of the a-axis AFM chains in Fig. 3. The configurations "+ +" and "− −" would have a given direction of the polarization (say, $b+$), while the other two "+ −" and "− +" would have the opposite ($b-$). Once the sample is poled in the $b+$ direction, the commensurate phase will contain "+ +" and "− −" regions *only*, alternating along the c axis. We speculate that the incommensurate phase contains variable mixtures of the other two configurations, with relative proportion and spacing being related to the incommensurability. This provides a simple explanation for the initial *reduction* of $|\mathbf{P}|$ on cooling below 25 K [7], and can lead, on further cooling, to a complete *reversal* of the polarization of the Mn sublattice.

In summary, we have shown that a strict correlation exists between the electric and magnetic transitions of $TbMn_2O_5$, as identified by Hur *et al.* [7], changes in its magnetic structure, and small lattice anomalies. These observations, together with a careful analysis of the magnetic symmetry, provide a plausible explanation of the unusually small ferroelectric polarization in $TbMn_2O_5$. In analogy with the well-known magnetic case, we propose that weak ferroelectricity in RMn_2O_5 arises from a canted antiferroelectric arrangement of the atomic displacement. The evolution of the spontaneous polarization and of the magnetic structure on cooling and as a function of applied field is interpreted in terms of phase coherence between magnetically ordered Mn^{4+}/Mn^{3+} layers.

We acknowledge the invaluable help of Juan Rodriguez-Carvajal and helpful discussions with Daniel Khomskii. Research at Rutgers was supported by the NSF-DMR-0405682.

[1] G. Buisson, Phys. Status Solidi A **17**, 191 (1973).
[2] C. Wilkinson, F. Sinclair, P. Gardner, J. B. Forsyth, and B. M. R. Wanklyn, J. Phys. C **14**, 1671 (1981).
[3] P. P. Gardner, C. Wilkinson, J. B. Forsyth, and B. M. Wanklyn, J. Phys. C **21**, 5653 (1988).
[4] A. Munoz, J. A. Alonso, M. T. Casais, M. J. Martinez-Lope, J. L. Martinez, and M. T. Fernandez-Diaz, Phys. Rev. B **65**, 144423 (2002).
[5] K. Saito and K. Kohn, J. Phys. Condens. Matter **7**, 2855 (1995), and references cited within.
[6] I. Kagomiya, S. Matsumoto, K. Kohn, Y. Fukuda, T. Shoubu, H. Kimura, Y. Noda, and N. Ikeda, Ferroelectrics **286**, 889 (2003).
[7] H. Hur, S. Park, P. A. Sharma, J. Ahn, S. Guha, and S.-W. Cheong, Nature (London) **429**, 392 (2004).
[8] T. Kimura, T. Goto, H. Shintani, K. Ishizaka, T. Arima, and Y. Tokura, Nature (London) **426**, 55 (2003).
[9] S. Kobayashi, T. Osawa, H. Kimura, Y. Noda, I. Kagomiya, and K. Kohn, J. Phys. Soc. Jpn. **73**, 1031 (2004).
[10] S. Kobayashi, T. Osawa, H. Kimura, Y. Noda, I. Kagomiya, and K. Kohn, J. Phys. Soc. Jpn. **73**, 1593 (2004).
[11] P. Chandra and B. Doucot, Phys. Rev. B **38**, 9335 (1988).
[12] O. Tchernyshyov, O. A. Starykh, R. Moessner, and A. G. Abanov, Phys. Rev. B **68**, 144422 (2003).
[13] J. Rodriguez-Carvajal, Physica (Amsterdam) **192B**, 55 (1993); GSAS, A. Larson, and R. B. Von Dreele, Los Alamos Report No. LAUR-86-748, Los Alamos National Laboratory, 1986.
[14] J. B. Goodenough, Phys. Rev. **100**, 564 (1955); J. Kanamori, J. Phys. Chem. Solids **10**, 87 (1959); P. W. Anderson, Solid State Phys. **14**, 99 (1963).